Metal-Organic Frameworks for the Trace Multiplexed Adsorption and Quantitation of 50 Per- and Polyfluoroalkyl Substances

Lisa Hua,[1] Marcello B. Solomon,[2] Deanna M. D'Alessandro,[2] and William A. Donald[1*]

[1]*School of Chemistry, University of New South Wales, Sydney, Australia*

[2]*School of Chemical and Biomolecular Engineering, University of Sydney, Sydney, Australia*

*Author to whom correspondence should be addressed:
Prof. William A. Donald
School of Chemistry
The University of New South Wales, Sydney
Sydney, NSW 2052
Australia
w.donald@unsw.edu.au

Abstract

Per- and polyfluoroalkyl substances (PFAS) are persistent environmental contaminants that pose significant health risks. With recent regulatory guidelines lowering safe drinking water advisory limits to parts-per-quadrillion (ppq) levels, the need for methods capable of detecting and quantifying many PFAS simultaneously in trace amounts has become increasingly critical. In this study, six metal-organic frameworks were evaluated as solid-phase extraction sorbents for multiplexed adsorption of PFAS, followed by quantitative liquid chromatography-tandem mass spectrometry. UiO-66 demonstrated the highest performance with 87% adsorption efficiency and 85% recovery for 33 PFAS spiked at 2 parts per billion. In multiplexed adsorption for 50 PFAS at concentrations of 200 ppq, UiO-66 achieved an average recovery of 75%, with detection limits as low as 4 ppq and an average detection limit of 108 ppq. Validation using six environmental water samples revealed quantifiable PFAS in all samples with 25 PFAS detected. Compared to polymeric resins, which typically detect PFAS in the 1–80 parts per trillion range, UiO-66 demonstrated enhanced sensitivity for multiplexed adsorption, capable of detecting concentrations in the low ppq range. These findings highlight the potential of UiO-66 for large-scale PFAS monitoring under increasingly stringent environmental regulations.

Introduction

Per- and polyfluoroalkyl substances (PFAS) are widely used in industrial applications, firefighting foams, and everyday products like non-stick cookware and food packaging.[1] PFAS are considered highly amphiphilic molecules consisting of hydrophobic 'tails' of inert C-F bonds and hydrophilic 'head' groups such as carboxylic acids, sulfonic acids, and sulfonamides.[2] This dual nature allows PFAS to spread easily in water and soil leading to their accumulation in ecosystems.[3] Of particular concern are compounds like perfluorooctanoic acid (PFOA) and perfluorooctanesulfonic acid (PFOS), which have been linked to serious health risks and were recently classified as carcinogens.[4] As the list of concerning PFAS grows, expanding monitoring efforts in water beyond just PFOA and PFOS is increasingly crucial.

Current commercial methods for PFAS detection often rely on solid-phase extraction (SPE) with polymer-based cartridges, which bind PFAS for later analysis by liquid chromatography tandem mass spectrometry (LC-MS/MS).[5] For PFAS preconcentration, weak anion exchange (WAX) cartridges with polymeric resins are commonly used to bind anionic PFAS and elute them with methanolic ammonium solutions.[6, 7] While effective, these approaches struggle to meet the increasingly stringent regulatory limits set by agencies like the US EPA, which now require detection at low parts per quadrillion (ppq) levels for compounds like PFOA and PFOS.[8]

To meet stricter detection requirements, there is growing interest in advanced materials for PFAS preconcentration.[9, 10] Metal-organic frameworks (MOFs), with their highly tunable structures and large surface areas (Figure 1), have emerged as promising alternatives to WAX materials for PFAS extraction and detection.[11-13] The first application of MOFs for PFAS adsorption was reported in 2015 with MIL-101(Cr) used to adsorb perfluorooctanoic acid (PFOA).[14] Since then, 15 MOFs—including MIL-101(Fe, Cr)[15, 16] ZIF-7,[17] ZIF-8,[17] SCU-8,[18] UiO-66,[19, 20] and NU-1000[21]—have been explored for their ability to adsorb PFAS. Earlier

work focused primarily on high concentrations of PFOA and PFOS for remediation applications.[13] Recently, Li et al. evaluated three MOFs (ZIF-8, UiO-66, and NU-1000) for PFAS removal from aqueous film forming foam (AFFF)-impacted water finding NU-1000 most effective, particularly for longer-chained PFAS, which can be removed from water at low concentrations (ppt).[21] NU-1000 could remove both anionic and non-ionic PFAS from water across a concentration range from 3.0 ppt to 250 ppb.

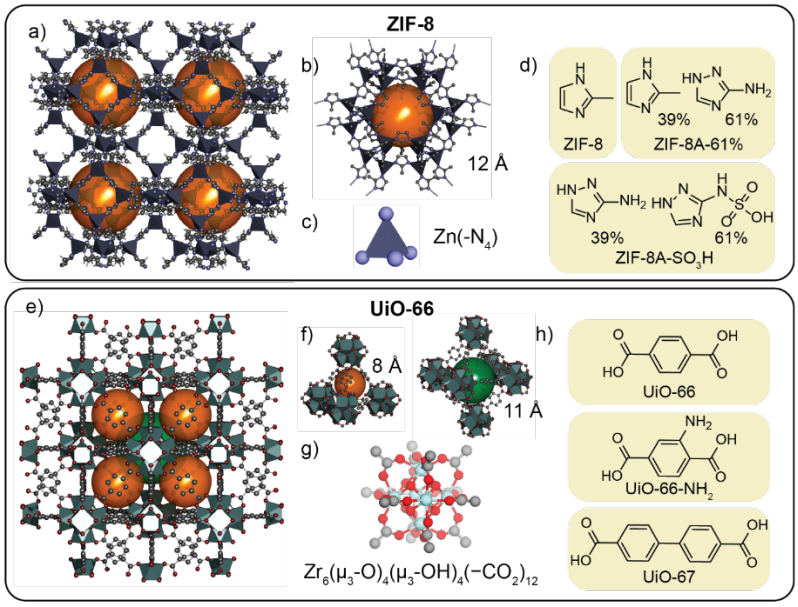

Figure 1. Structural characteristics of metal-organic frameworks (MOFs) used for multiplexed quantitation of 50 PFAS at trace levels from water. The figure illustrates the structures of ZIF-8 and UiO-66 MOFs, emphasizing pore size, unsaturated metal nodes, and functional groups. (a) ZIF-8 crystal structure with the main pore cavity shown in orange, (b) pore diameters of 12 Å for ZIF-8, (c) metal-binding node of ZIF-8 [Zn(-N_4)], (d) linker ligands used for synthesizing ZIF-8 analogs with $ZnNO_3 \cdot 6H_2O$, (e) UiO-66 crystal structure with pore cavities in orange and green, (f) two main pore cavities of UiO-66 with diameters of 8 Å and 11 Å, (g) metal-binding node of UiO-66 [$Zr_6(\mu_3\text{-}O)_4(\mu_3\text{-}OH)_4(CO_2)_{12}$], and (h) linker ligands for UiO-66 analogs synthesized with $ZrCl_4$. Atoms are represented as follows: Zn (purple tetrahedra), C (grey), N (blue), O (red), and Zr (light blue). Hydrogen atoms are omitted for clarity.

Previous research on MOFs and PFAS has largely centered on their adsorption mechanisms and effectiveness in PFAS remediation. However, the use of MOFs to enhance PFAS detection in water—where high sensitivity at trace concentrations is essential—remains relatively unexplored. Donald and colleagues have previously demonstrated the potential of ZIF-8 in MOF-based solid-phase microextraction probes, achieving detection limits as low as 11 ppt for PFOA.[22] Additionally, Jia et al. reported detection limits of low to sub-ppt for 9 PFAS

using a dual-functional MIL-101(Cr) MOF in combination with liquid chromatography tandem mass spectrometry (LC-MS/MS).[23] MOF-based solid-phase extraction methods, such as those employing UiO-66-F_4 and MOF-5, have also shown promise for preconcentrating PFAS, with detection limits of 2.6 ppt for PFOA and 70 ppt for PFOS, using laser desorption ionization or gas chromatography-mass spectrometry (GC-MS).[24-26] While these early studies highlight the promise of MOFs for detecting PFAS, the focus has typically been on a limited number of anionic PFAS, primarily in controlled conditions, and scarce use of quantitative LC-MS/MS, the 'gold standard' for accurate PFAS quantitation with isotopically labeled standards.

In this study, we address key challenges in PFAS detection by use of multiplexed PFAS adsorption with MOFs to achieve low parts-per-quadrillion (ppq) detection limits through quantitative LC-MS/MS. Six MOFs were evaluated for their adsorption efficiency across 33 PFAS, with six elution solutions tested to optimize recovery. UiO-66 emerged as the most effective, and its performance was compared to ZIF-8 for the multiplexed adsorption of 50 PFAS, including zwitterionic (6:2 FTAB), cyclic (PFECHS), and chlorinated (9Cl-PF3ONS, 11Cl-PF3OUdS) species at concentrations of 200 ppq and 20 ppt. The method was applied to environmental water samples from Sydney, Australia. This approach broadens the scope of PFAS detected using MOFs, enhancing both sensitivity and real-world applicability of MOF-based detection technologies.

Results and Discussion

Materials selection and characterization. Six MOFs from two MOF families (ZIF-8 and UiO-66) were chosen for investigation (Figure 1). These materials can be readily synthesized in gram-scale quantities,[27, 28] are stable in water samples across a broad range of pH values,[29, 30] contain different functional groups capable of anion and cation exchange (amines and sulfonic acids) and a wide range of pore sizes (8 – 22 Å). In Figure 1b and f, the pore structures of the two MOF families are shown. These MOFs have distinct structural

characteristics that influence their molecular adsorption characteristics. ZIF-8, composed of zinc ions and 2-methylimidazolate ligands, has a zeolite-like sodalite structure with high porosity and large pore windows. In contrast, UiO-66 consists of zirconium oxide clusters (Figure 1g) and terephthalate ligands, forming a robust face-centered cubic lattice with smaller, stable pores. Using different organic linkers (Figure 1d and h) while maintaining the same general framework shape can significantly alter the pore characteristics, such as size, shape, and surface functionality, which in turn affects their adsorption properties, stability, and molecular adsorption properties. For example, the incorporation of extra functional groups, larger ligands and tailored defect sites can incorporate amines (ZIF-8A-61%, UiO-66-NH_2) and sulfonic acid (ZIF-8A-SO_3H) groups into the pores and create materials with larger pores (UiO-67 and defective UiO-66).

The six MOFs of interest were synthesized using literature methods and characterized by use of BET and PXRD experiments (Table S1 and Figure S1). The surface areas, pore sizes and the crystalline diffraction patterns were consistent with previously reported data for these six materials, with measured surface areas within 10% of literature data (20% for ZIF-8A-61%)[27, 31-37] and powder diffraction results were in reasonable agreement with characteristic Bragg reflection positions calculated from crystal structures.[35, 38] For ZIF-8A-61%, NMR was used to confirm and quantify the partial conversion of the methylated ZIF-8 ligand, 2-methylimidazole, to the aminated 3-amino-1,2,4-triazole found in ZIF-8A with a yield of ~61% (Figure S2), consistent with previous research reported in the literature.[31]

UiO-66 was synthesized with a range of defect states (e.g. missing linkers and cluster sites) and characterized by BET, PXRD and TGA experiments (Table S2, Figure S3-4). The surface areas and pore sizes from BET measurements are consistent with defective materials containing pore sizes of 8, 11, 16, and 18.5 Å, with defective free UiO-66 containing only pore sizes of 8 and 11 Å. With the addition of increasing amounts of HCl, the surface area decreases

while the distribution of pore sizes shifts towards the larger pore sizes, which agrees with results reported by Clark et al. based on BET measurements (Table S2).[19] The measured powder diffraction patterns agreed with the simulated patterns out to high angle peaks (2θ beyond 30°) which ensures that crystalline structures were synthesized. Results from TGA (Figure S4) were used to approximate the number of defects present in these materials. Using a procedure reported by Lillerud and co-workers,[39] UiO-66-5, UiO-66-10 and UiO-66-25 are respectively missing ~0.76, ~0.81 and ~1.51 out of 6 linkers per Zr_6 formula unit that is expected for the pristine MOF, which are comparable or slightly lower than previously reported by Clark et al.[19]

Assessing the analytical capabilities of different MOFs. The structures of the initial 33 PFAS that were measured are shown in Figure 2a, arranged in order of increasing chain length for each functional head group (carboxylic acids, sulfonic acids, sulfonamides, and fluorotelomers). The analytical capabilities of the six chosen MOFs were assessed in their performance for the adsorption and elution of 33 PFAS using MOFs as dispersive solid-phase extraction (dSPE) sorbents, with quantitative isotope dilution LC-MS/MS. The overall results of the adsorption and elution testing are summarized in Figure 2b as a bubble plot, in which the extent of adsorption of PFAS is indicated in dark purple and the extent of elution in light purple, with larger circles representing higher extents of adsorption or elution for each PFAS using each MOF. Detailed individual PFAS adsorption and elution performance by ZIF-8 and UiO-66 analogs is shown in Figure S5 and S6. Throughout this work, the process of removing PFAS from water using MOFs will be referred to as an adsorption process, although there are likely absorption processes occurring particularly for shorter chain PFAS. When comparing the six MOFs tested for their PFAS adsorption capabilities, it was found that ZIF-8A-SO_3H, UiO-66, and UiO-67 adsorb PFAS most effectively with the highest average amount of all 33 PFAS removed (85%, 87%, and 99% respectively; Table S3). Moreover, UiO-66 has the highest amount adsorbed and eluted (85%) compared to UiO-67 (80%), ZIF-8A-SO_3H (75%), ZIF-

8A-61% (69%), UiO-66-NH_2 (62%) and ZIF-8 (46%). UiO-66 elutes 13 individual PFAS above 90%, and for each individual PFAS, UiO-66 has higher extents of elution than any of the other five MOFs tested for the vast majority of PFAS (p-value < 0.05) (Table S3). These data suggest that UiO-66 is the most effective of these MOFs for the adsorption and elution across all 33 PFAS under these conditions.

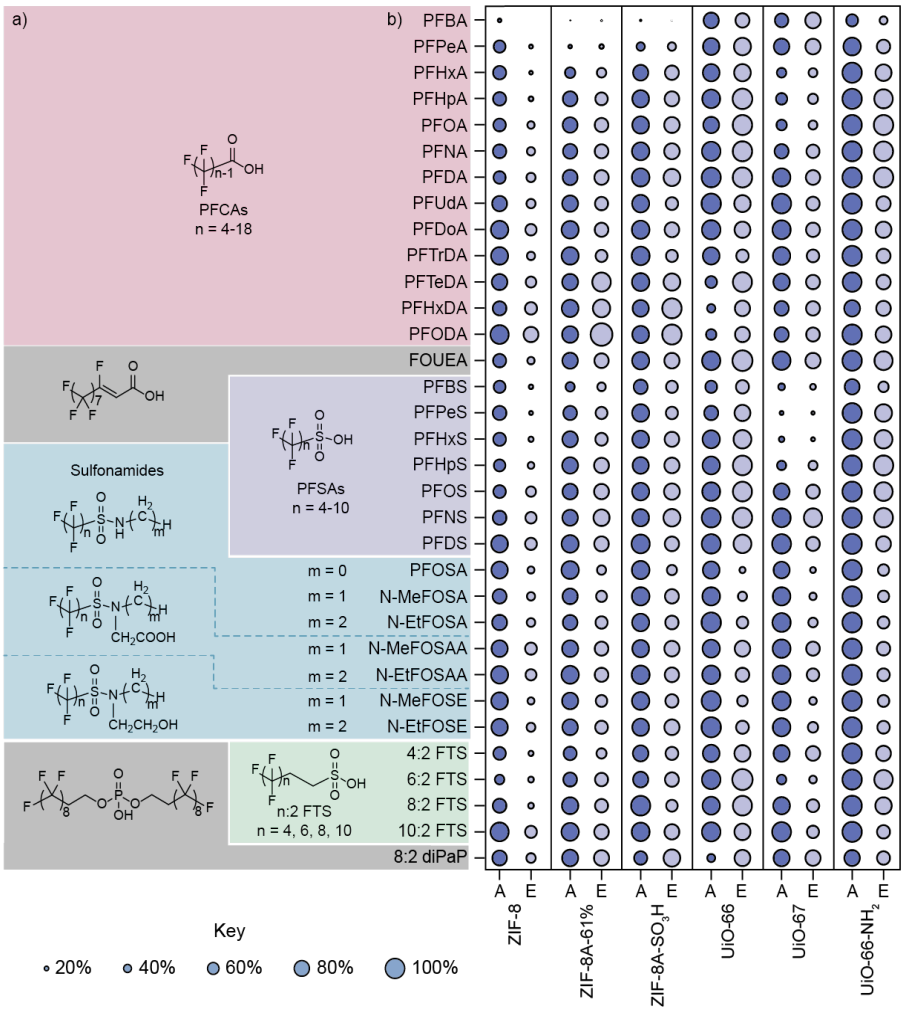

Figure 2. The extent of PFAS extraction from water using MOFs and PFAS elution from MOFs depends on the identity of the MOF, the PFAS head group and the chain length. (a) 33 perfluoroalkyl substances (PFASs) of environmental concern including 13 perfluorocarboxylic acids (PFCAs), seven perfluorosulfonic acids (PFSAs), seven sulfonamides, four fluorotelomer sulfonic acids (n:2 FTS) and two longer chained PFAS (FOUEA and 8:2 diPaP, black). (b) Extent of PFAS adsorption (A) from water for each MOF, and extent of PFAS elution (E) from each MOF using methanolic solutions. The size of the circles corresponds to the amount of PFAS that is absorbed and eluted. Refer to Figure S5 and S6 for the 95% confidence intervals which are on average ±4% of the measured recovered values for adsorption values and ±5% of the measured recovered values for the elution values across all 198 individual recovery values.

Although UiO-66 was chosen for further investigations to lower detection limits for PFAS, the adsorption and elution of sulfonamides remains poor. For an effective adsorbent-molecule pair, strong interactions between the molecule and the adsorbent material are beneficial and should be stronger than the interactions with water. For effective elution, the molecule should also have strong interactions with the elution solvent. Additionally, factors including entropy changes, pore size, and structure can also have important roles. Sulfonamides such as PFOSA, N-MeFOSA, and N-EtFOSA have higher p*K*a values than the carboxylic and sulfonic acid PFAS and are less ionized, reducing the extent of ionic interactions between the positively charged MOF scaffold and the sulfonamide PFAS. However, UiO-66 has higher performance for the adsorption and elution of short-chained PFAS, which is of particular relevance in current detection efforts as polymeric materials tend to have low recoveries for these compounds.

To further optimize the UiO-66 material, pristine and defective UiO-66 materials were explored to optimize multiplexed PFAS adsorption from water. Here, four materials were tested, UiO-66-X (X = 0, 5, 10 and 25, where *X* represents the volume percent of HCl concentration added during synthesis to form defect sites, and X = 0 denotes nearly defect free UiO-66). The average adsorption and elution of 33 PFAS for these UiO-66 materials is shown in Table S4. The highest overall average adsorption and elution of PFAS occurs with UiO-66-5. The majority of PFAS are recovered to a greater extent with UiO-66-5 than UiO-66-0, UiO-66-10, and UiO-66-25 (*p*-values < 0.05; Table S4). UiO-66-5 likely has the optimal combination of pore sizes and abundance for PFAS to be effectively adsorbed by the material, and these data supports previous findings by Clark et al. where some defectivity in UiO-66 increases the uptake of PFAS.[19] Here, UiO-66-5 was the most effective UiO-66 material tested leading to its use in further experiments.

Lastly, the elution conditions used to extract PFAS from UiO-66 following adsorption were validated by testing six different elution solvents (Table S5). These six solutions were chosen to compare previous solutions in literature that regenerate their materials for further testing. The use of methanolic solutions was found to significantly increase the recovery of PFAS from UiO-66-5 compared to aqueous solutions. The extent of recovery slightly increases with the addition of additives such as ammonia, NaCl and HCl. Thus, methanolic solutions were used to elute PFAS in all further experiments.

Overall, these results provide a comprehensive comparison of six different MOFs for LC-MS/MS analysis of 33 PFAS, demonstrating the superior performance of UiO-66, particularly for short-chained PFAS (Figure 2). Previous research has utilized MOFs as dispersive solid-phase extraction sorbents, analyzed by MALDI-TOF-MS, GC-MS, or SALDI-MS, focusing on seven MOFs tested for either PFOA or PFOS.[24-26] The results presented here provide a direct comparison between MOFs at low concentrations for a broad range of PFAS using a quantitative isotope dilution targeted LC-MS/MS method.

Multiplexed screening of 50 PFAS at ultra-trace concentrations using MOF sorbents. To further evaluate UiO-66 as a dSPE material for analyzing PFAS concentrations in aqueous samples, the PFAS screen was expanded from 33 to 50 compounds. These additional PFAS include HFPO-DA (Gen-X) and PFEESA which contain alkoxy groups, shorter and longer-chained sulfonic acids (PFPrS, PFDoS), fluorotelomers (n:3 FTCA), other phosphoric acids (6:2 diPAP, 6:2/8:2 diPAP), cyclic PFAS (PFECHS), chlorinated PFAS (9Cl-PF3ONS and 11Cl-PF3OUdS), and 6:2 FTAB, a zwitterionic PFAS. Most of these PFAS have been introduced to replace longer-chained PFAS such as PFOA and PFOS and may potentially be less toxic.[40] Additionally, some are potential degradation products (PFPrS) or longer-chained PFAS previously used in industry (PFDoS). Apart from 5:3 FTCA (FPePA), these PFAS have not been previously tested for adsorption or elution by MOFs.

Both UiO-66 and ZIF-8 were tested, as ZIF-8 has been used previously for analyzing PFOS of the three ZIF-8 analogs, using laser desorption to quantify concentrations.[24] The tests were conducted at 200 ppq, the lowest reported spike concentration of PFAS in any dSPE MOF method to date. Extracted ion chromatograms (Figure 3a-f) indicate that UiO-66 can be used to detect all PFAS, while ZIF-8 detected only half with a signal-to-noise (*S*/*N*) ratio greater than 3.

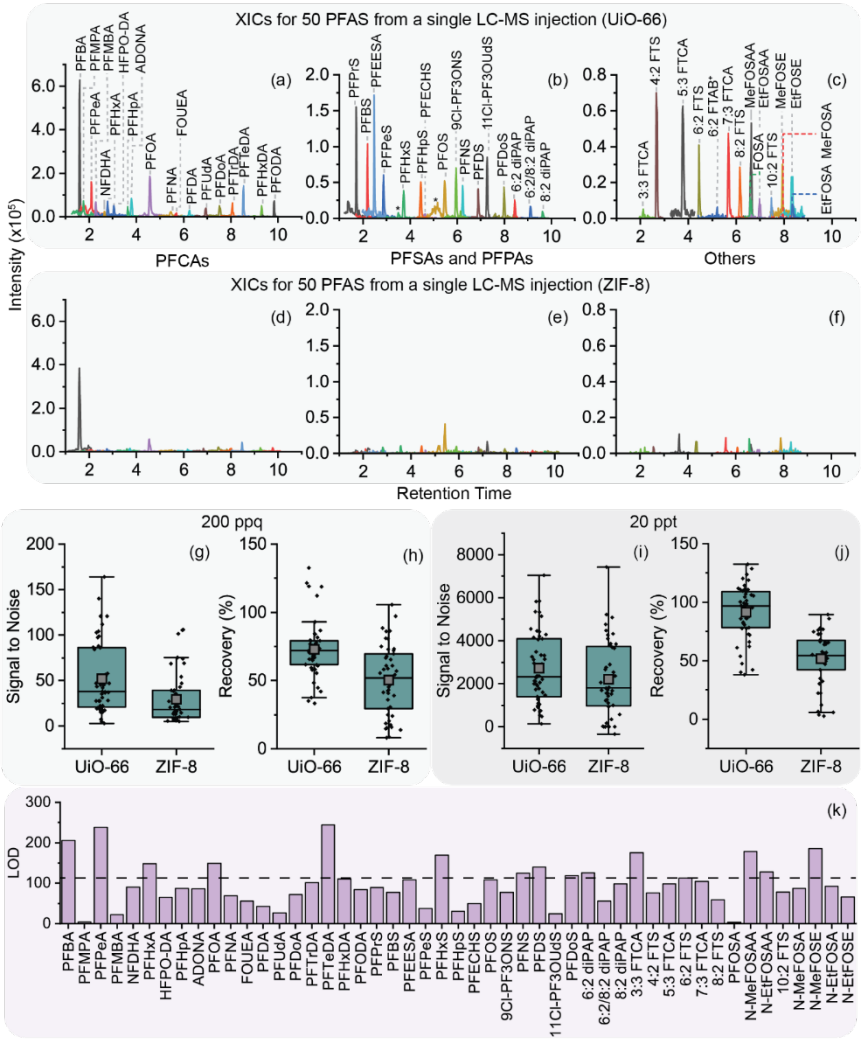

Figure 3: UiO-66 outperforms ZIF-8 analytical performance at low concentrations. (a)-(f) shows chromatograms of the recovery of a 50 PFAS 200 ppq spike using UiO-66 ((a)-(c)) or ZIF-8 ((d)-(f)) as dSPE sorbent and are shown by functional group: (a) and (d) show the perfluorocarboxylic acids (PFCAs), (b) and (e) show perfluorosulfonic acids (PFSAs) and perfluorophosphoric acids (PFPAs) (* represents the branched components of PFHxS and PFOS, linear PFHxS and PFOS labelled) and (c) and (f) show the fluorotelomers (n:2 FTS and n:3 FTCA), sulfonamides and zwitterionic PFAS (6:2 FTAB chromatogram shown at 2 ppb). (g) average individual PFAS signal to noise (*S*/*N*) value for 50 PFAS and (h) percentage recovery of a 200 ppq spike, (i) average individual PFAS signal to noise (*S*/*N*) value for 50 PFAS and (j) percentage recovery of a 20 ppt spike. (k) LOD values for 50 PFAS with the average shown as a dotted line, PFAS organized by functional group by order of retention time.

At 200 ppq, UiO-66 exhibited higher average *S*/*N* for all 50 PFAS (52) than ZIF-8 (30) (Figures 3g and S7). Moreover, the average recovery across all PFAS at 200 ppq for UiO-66 (73%) was also higher than ZIF-8 (51%) (Figures 3h and S8, Table S6). Testing at 2 ppb also showed higher percentage recovery with UiO-66 (Figure 2), and similar trends were observed at 20 ppt (Figures 3i and 3j, Table S6, Figure S7-8). For example, UiO-66 demonstrated nearly 100% recovery on average across all 50 PFAS at 20 ppt, while ZIF-8 was considerably lower (50%). Moreover, XRD patterns indicated that the MOFs' crystalline structures remained intact post-PFAS adsorption, demonstrating stability (Figure S9).

With UiO-66 showing promise as a pre-concentration sorbent, the limit of detection (LOD) was determined for 50 PFAS (Figure 3k and Table S7) by constructing calibration curves with PFAS solutions from 200-800 ppq, with representative PFAS calibration curves shown in Figure S10. These calibration curves had average regression values of 0.97, indicating linearity. The average LOD for 50 PFAS using our dSPE method was 108 ppq, and average LOQ was 362 ppq. These detection limits are lower than previous dSPE methods using MOFs, where the use of UiO-66-F_4 as a dSPE sorbent had a LOD of 2.6 ppt for PFOA.[25] For methods that quantify more than 40 PFAS, the lowest LODs achieved are in the low ppt range, tested at 2000 ppt.[41] In addition to anionic PFAS tested in negative ionization mode, 6:2 FTAB, a zwitterionic PFAS, in positive ionization mode was also measured using the reported dSPE MOF method. 6:2 FTAB, a replacement for PFOS in firefighting foams, was detected and quantified using a MOF for the first time. Although not detectable at 200 ppq, 6:2 FTAB was detected at concentrations above 0.4 ppt, with quantification limits at 1.3 ppt. Overall, UiO-66 outperformed ZIF-8 as a dSPE sorbent in average recovery and higher *S*/*N* ratios, with lower limits of detection across 50 PFAS, while retaining stability post-adsorption.

UiO-66 for the multiplexed detection of PFAS from environmental water samples. The efficacy of the UiO-66 dSPE method was tested using environmental water samples collected from various locations around Sydney. Six different water samples with different matrices were collected: chlorinated water (Marrickville), tap water (North Ryde), beach water (Kyeemagh), river water (North Richmond), lagoon water (Richmond), and water from Engine Pond near Sydney Airport (Mascot). The latter site is a known site of PFAS contamination owing to the extended legacy of using aqueous film forming foam (AFFF) in firefighting exercises. The locations are shown on a map in the Supporting Information (Figure S11). The concentrations and their internal recoveries of each PFAS are given in Figure 4 and Table S8 respectively. Out of the 50 PFAS tested, 25 PFAS were detected across the six samples above the limit of quantification (LOQ; Figure 4 and Table S8). Internal standard recoveries were acceptable (between 70-120%) for most samples, indicating accurate quantification of PFAS (Table S8). However, lower recoveries of the shortest-chained PFCAs (PFBA, PFPeA, PFHxA, PFHpA, and PFOA) in the beach water sample were consistent with competitive binding between PFAS and high concentrations of counterions in the ocean water sample. To investigate the impact of counterions on PFAS recovery, tap water samples were spiked with different acids (HCl, CH_3COOH, H_2SO_4, and H_3PO_4) to introduce different anions into the solution (Table S9). Focusing on the recovery of PFCAs (Figure S12) the addition of HCl did not decrease the percentage recovery of internal standards, as Cl^- counterions are already present in the UiO-66 structure from synthesis and do not bind to additional sites. This observation aligns with previous findings by Clark et al., which also noted that Cl^- at 25 mg/L does not decrease PFAS adsorption by UiO-66.[19] However, the study found that with increasing net charge of the added anion, the adsorption of the shortest-chained PFAS by UiO-66 decreased (in the order of $CH_3COO^- > SO_4^{2-} > PO_4^{3-}$). Sulfate and carbonate anions have been shown to competitively bind to sites occupied by PFAS.[12] Our current findings support this notion and indicate that the

presence of more highly charged counterions is a key factor in the reduced adsorption of short-chain PFCAs. Overall, these results demonstrated the potential for MOFs to be used for the effective preconcentration and analysis of PFAS at ultra-trace levels in environmental water samples.

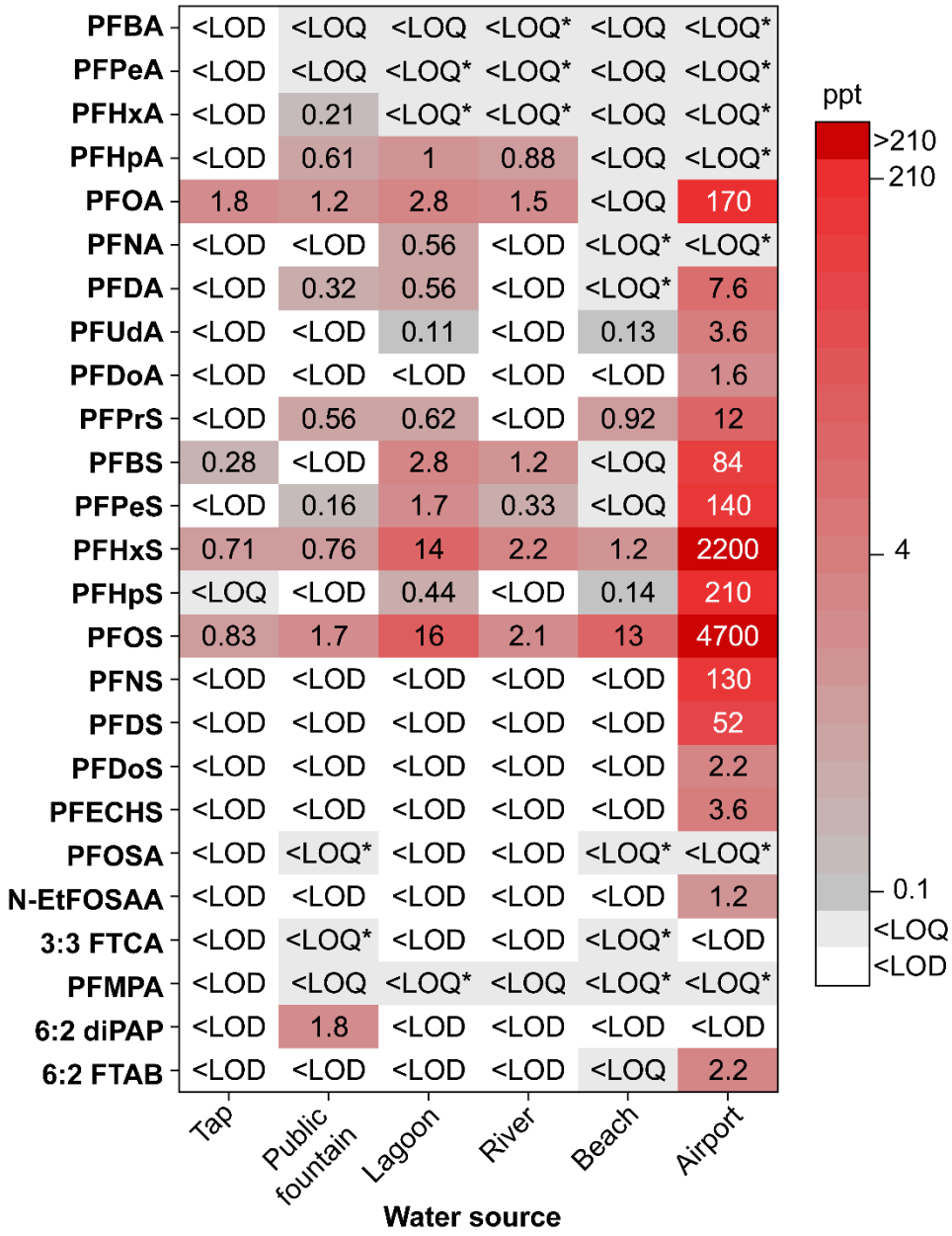

Figure 4: Multiplexed quantification of 50 PFAS in six different water matrices using UiO-66 sorbent and LC-MS/MS. Refer to Figure S11 and Table S8 for a map of the water collection sites and internal standard recoveries respectively. Values are reported in ppt. Only PFAS that were detected above the LOD are shown in the table. <LOD indicates that the concentration of PFAS was below detection limits, <LOQ indicates that concentration of that PFAS is below the limit of quantification but above LODs. <LOQ* indicates that the concentration of PFAS is above the limit of detection, however internal standard recoveries were not between 70-120%.

Experimental Methods

Materials, reagents and samples. Full details of all materials, reagents, and solvents are provided in the Supporting Information. IUPAC names for all PFAS investigated are shown in Table S10. Environmental water samples were collected in triplicate from around the Sydney basin area (locations shown in Figure S11) in 500 mL polypropylene sample bottles, which were stored at 4 °C prior to analysis. The sample (250 mL) was decanted into a separate polypropylene (500 mL) before analysis by dSPE UiO-66 within 5 d of collection.

Preparation of MOFs. ZIF-8 and UiO-66 analogs were synthesized using established literature methods with slight modifications. Full synthetic procedures and characterization details are provided in the Supporting Information (SI). Briefly, ZIF-8 and ZIF-8 analogs ZIF-8A-61% and ZIF-8A-SO_3H were prepared via the reaction of zinc nitrate hexahydrate and 2-methylimidazole in methanol, followed by post-synthetic modifications with 3-amino-1,2,4-triazole (ZIF-8A-61%) and 1,3-propanesultone (ZIF-8A-SO_3H).[31] UiO-66 and UiO-66 analogs UiO-66-NH_2 and UiO-67 were synthesized by reacting zirconium chloride with the corresponding organic ligand in DMF, with defect engineering for UiO-66 achieved by varying the amount of HCl during synthesis. Characterization data (e.g., PXRD and BET surface area) were in agreement with literature reports.

Materials characterization. Powder X-ray diffraction (PXRD) was performed using a PANanalytical X'Pert PRO Diffractometer with Cu-Kα radiation (λ = 1.5406 Å), scanned at 45 kV, 40 mA with a step size of 2θ = 0.026° over 4 to 50°. Adsorption isotherms were measured using a 3-Flex Surface Area and Pore Size Analyzer (Micromeritics). Samples (30-50 mg) were outgassed at 150 °C under vacuum for 24 h. Brunauer-Emmett-Teller (BET) surface areas were determined from N_2 isotherms at 77 K using density functional theory modeling for pore size distribution.[42] Thermogravimetric analysis (TGA) was conducted on a TA Discovery Analyzer under dry air (20 mL/min), heating at 5 °C/min from 40 to 700 °C. ^{1}H and ^{13}C NMR spectra

were recorded at 298 K on a 400 MHz Bruker Avance III HD system by dissolving 5 mg of the MOF in d_6-DMSO (0.5 mL) with concentrated sulfuric acid (0.05 mL, 98%). Ligand conversion was monitored by comparing peaks of 2-methylimidazole (δ = 7.4 ppm) and 3-amino-1,2,4-triazole (δ = 8.2 ppm).

Quantification of PFAS adsorption and elution for six MOFs. PFAS adsorption by six MOFs was evaluated using a 33 PFAS methanol spike solution (100 ppb), prepared from standards (Table S10) spiked into water to obtain 2 ppb of each PFAS. Tested elution solvents included water, methanol, 80/20 methanol/water (v/v), 0.4% ammonia/methanol (v/v), 0.1 M HCl/methanol (30/70 v/v), and 0.05 M NaCl/methanol (30/70 v/v). MOFs (10 mg) were activated at 95 °C for 5 h, then added to 10 mL of the spiked water solution (pH 4) and agitated for 30 min (1 rpm/s). After centrifugation (2800 rpf, 5 min), the supernatant (0.5 mL) was filtered (0.22 μm nylon membrane) with centrifugation at 1100 rpf for 5 min. The membrane was cleaned with 0.4% MeOH/NH_4 (0.5 mL), followed by LC-MS/MS analysis. PFAS adsorption by the MOFs was quantified by subtracting the PFAS concentration after adsorption from a blank sample and comparing it to a control without MOF. Elution was performed by decanting water from the MOF pellets, adding 10 mL of elution solvent, agitating for 30 min (1 rpm/s), and centrifuging (1650 rpf, 5 min). The filtered supernatant (1 mL) was analyzed by LC-MS/MS to determine elution efficiency. Full details regarding the quantification of the extent of adsorption and elution are in the Supporting Information.

PFAS solutions for limit of detection testing. A 50 PFAS methanol spike solution at 100 ppb was prepared by combining Wellington Laboratories standards PFAC-MXF, PFAC-MXG, PFAC-MXH, PFAC-MXJ, with 12 individual PFAS standards (Table S10). A 27 isotopically labelled PFAS internal standard solution at 100 ppb was prepared by combining Wellington Laboratories standards MPFAC-24ES, with 8 individual isotopically labelled PFAS standards (Table S11). A 4 PFAS recovery standard solution containing isotopically labelled standards at

20 ppb was prepared using Wellington Laboratories standard MPFAC-C-IS (M3PFBA, M2PFOA, MPFDA, MPFOS) to determine the percentage of internal standards recovered at the end of extraction.

Protocol for using dSPE with MOFs for ultra-trace PFAS analysis. Water (~ 250 mL) containing the 50 PFAS mixture spiked at 100, 200, 400, 600 or 800 ppq (or environmental water samples) was placed in a polypropylene container. The 27 PFAS internal standard solution (10 µL, 100 ng/mL) was added, followed by HCl (1 mL, 0.5 M) or alternative acids (CH_3COOH, 1 mL, 0.4 N; H_2SO_4, 2.5 mL, 0.2 N; H_3PO_4, 1.5 mL, 2%) to adjust pH to 3-4. The MOF (100 mg) was dispersed in the water and agitated for 1 h at 0.5 rpm/s. After filtration through a 0.22 µm nylon membrane using a polysulfone bottle top filter, the MOF was transferred to a 15 mL tube, dried with nitrogen gas for 15 min, and eluted with 0.4% ammonia methanol (8 mL) for 30 min at 1 rpm/s. The solution was centrifuged (1650 rpf, 5 min) and the supernatant methanol was concentrated to 2-3 mL with nitrogen at 40 °C. Milli-Q water (0.25 mL) was added to prevent peak splitting, and the extract was further concentrated to 1 mL. After adding a recovery standard (50 µL), the solution was filtered through a 0.22 µm nylon filter and transferred to a 700 µL vial for LC-MS/MS analysis.

Mass spectrometry. A multiple reaction monitoring experiment was conducted in negative ionization mode using LC-MS/MS (ExionLC AD-SciEx Triple Quad 6500+) with a C18 column (Waters Acquity UPLC BEH or Phenomenx Luna Omega, both 50 x 2.1 mm, 1.6–1.7 µm). Quantification was performed using a ten-point calibration (0.025–25 µg/L) with isotopically labeled internal standards (Table S11). The sample injection volume was 5 µL and full details of LC-MS/MS parameters are detailed in Tables S12-S14. PFAS were quantified using internal standards when recoveries were between 70–120%, and results were reported only when PFAS exceeded the LOQ. LOD and LOQ were calculated from five-point calibration curves (100-800 ppq). Recoveries for 50 PFAS were compared between sorbent-

treated samples and direct injections. Further details are available in the Supporting Information.

Conclusions

UiO-66 demonstrated the highest performance across both average adsorption (87%) and recovery (85%) for 33 PFAS spiked in water at 2 ppb. Remarkably, at 200 ppq— the lowest concentration tested for any MOF in the literature—UiO-66 maintained an average recovery of 75% across 50 PFAS outperforming MOFs like ZIF-8. Optimization of defect sites on UiO-66 found that UiO-66-5, treated with 5% HCl, provided the optimal balance for PFAS adsorption. This balance likely arises from the creation of additional and larger pores while still maintaining enough structural integrity to effectively trap and retain PFAS molecules. The developed multiplexed adsorption protocol, coupled with quantitative isotope dilution LC-MS/MS, enabled a direct, first-of-its-kind performance comparison between MOFs at ultra-trace PFAS concentrations across a broad range of 50 PFAS including zwitterionic compounds such as 6:2 FTAB. Detection limits reached as low as 4 ppq, with an average LOD of 108 ppq. When applied to environmental water samples, UiO-66 was used to detect PFAS contamination in all samples with 22 PFAS identified in the most affected sample from Sydney Airport. Internal standard recoveries ranging from 70% to 120% ensured the accuracy and reliability of PFAS quantitation by correcting for variability in sample preparation and matrix effects, with nearly 100% recovery observed across all 50 PFAS for UiO-66. In contrast, ZIF-8 showed considerably lower recovery rates. The study also explored the effect of counterions, finding that higher-charged counterions (SO_4^{2-}, PO_4^{3-}) reduced adsorption of short-chain PFAS, while Cl^- had essentially no effect. Importantly, UiO-66 retained its crystalline structure post-adsorption, confirming its stability for practical use. Overall, UiO-66 is a highly effective MOF for PFAS detection, demonstrating superior recovery, structural integrity, and sensitivity down

to low ppq. This study highlights UiO-66's potential for comprehensive environmental monitoring particularly for zwitterionic and cationic PFAS.

Acknowledgements

We gratefully acknowledge the National Measurement Institute (NMI) and the Australian Research Council (FT200100798) for their support of this work. We also extend our thanks to Daniel Slee, Sam Falvey, Michelle Yu, and Dr. Deni Taleski (NMI) for their valuable discussions, the provision of standards, and access to instrumentation. We acknowledge Dr. Hyun Eui Lee (UNSW Sydney) for their early contributions to this project.

Table of Contents Graphic and Synopsis

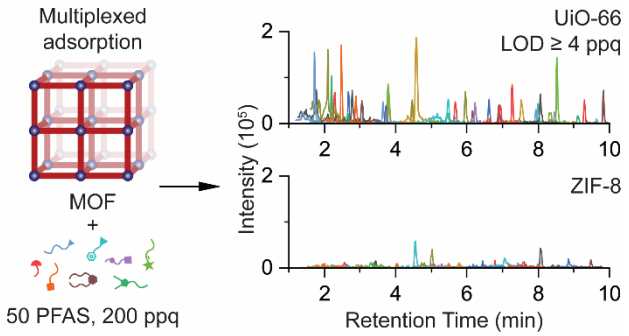

Multiplexed adsorption of 50 PFAS at low parts-per-quadrillion levels using UiO-66 enables high recovery in ocean and other environmental water samples, outperforming ZIF-8 for monitoring.

References

(1) Glüge, J.; Scheringer, M.; Cousins, I. T.; DeWitt, J. C.; Goldenman, G.; et al. An overview of the uses of per- and polyfluoroalkyl substances (PFAS). *Environ. Sci. Process. Impacts* **2020**, *22*, 2345-2373. DOI: 10.1039/D0EM00291G.
(2) Kwiatkowski, C. F.; Andrews, D. Q.; Birnbaum, L. S.; Bruton, T. A.; DeWitt, J. C.; et al. Scientific Basis for Managing PFAS as a Chemical Class. *Environ. Sci. Technol. Lett.* **2020**, *7* (8), 532-543. DOI: 10.1021/acs.estlett.0c00255.
(3) Parolini, M.; Felice, B. D.; Rusconi, M.; Morganti, M.; Polesello, S.; et al. A review of the bioaccumulation and adverse effects of PFAS in free-living organisms from contaminated sites nearby fluorochemical production plants. *Water. Emerg. Contam. Nanoplastics.* **2022**, *1* (18). DOI: 10.20517/wecn.2022.15.
(4) Zahm, S.; Bonde, J. P.; Chiu, W. A.; Hoppin, J.; Kanno, J.; et al. Carcinogenicity of perfluorooctanoic acid and perfluorooctanesulfonic acid. *Lancet Onol.* **2024**, *25* (1), 16-17. DOI: 10.1016/S1470-2045(23)00622-8.
(5) U.S. Environmental Protection Agency, Shoemaker, J and Tettenhorst, D. Method 537.1 Determination of Selected Per- and Polyfluorinated Alkyl Substances in Drinking Water by Solid Phase Extraction and Liquid Chromatography/Tandem Mass Spectrometry (LC/MS/MS). U.S. Environmental Protection Agency, Washington, DC, 2020. https://cfpub.epa.gov/si/si_public_record_report.cfm?dirEntryId=348508&Lab=CESER&simpleSearch=0&showCriteria=2&searchAll=537.1&TIMSType=&dateBeginPublishedPresented=03%2F24%2F2018 (accessed 2024-09-25)
(6) Boyer, T. H.; Fang, Y.; Ellis, A.; Dietz, R.; Choi, Y. J.; et al. Anion exchange resin removal of per- and polyfluoroalkyl substances (PFAS) from impacted water: A critical review. *Water Res.* **2021**, *200* (117244). DOI: 10.1016/j.watres.2021.117244.
(7) Dixit, F.; Dutta, R.; Barbeau, B.; Berube, P.; Mohseni, M. PFAS removal by ion exchange resins: A review. *Chemosphere* **2021**, *272* (129777). DOI: 10.1016/j.chemosphere.2021.129777.
(8) U.S. Environmental Protection Agency, *PFAS National Primary Drinking Water Regulation.* U.S. Environmental Protection Agency, Washington, DC, 2020. https://www.epa.gov/system/files/documents/2024-04/pfas-npdwr_fact-sheet_general_4.9.24v1.pdf (accessed 2024-09-25)
(9) Li, D.; Londhe, K.; Chi, K.; Lee, C.-S.; Venkatesan, A. K.; et al. Functionalized bio-adsorbents for removal of perfluoroalkyl substances: A perspective. *AWWA Wat. Sci.* **2021**, *3* (6). DOI: 10.1002/aws2.1258.
(10) Gomri, C.; Benkhaled, B. T.; Cretin, M.; Semsarilar, M. Adsorbent Material Used for the Treatment of Per- and Poly-Fluoroalkyl Substances (PFAS): A Short Review. *Macromol. Chem. Phys.* **2024**, *225* (11). DOI: 10.1002/macp.202400012.
(11) Karbassiyazdi, E.; Kasula, M.; Modak, S.; Pala, J.; Kalantari, M.; et al. A juxtaposed review on adsorptive removal of PFAS by metal-organic frameworks (MOFs) with carbon-based materials, ion exchange resins, and polymer adsorbents. *Chemosphere* **2023**, *311*. DOI: 10.1016/j.chemosphere.2022.136933.
(12) Li, R.; Adarsh, N. N.; Lu, H.; Wriedt, M. Metal-organic frameworks as platforms for the removal of per- and polyfluoroalkyl substances from contaminated waters. *Matter* **2022**, *5* (10), 3161-3193. DOI: 10.1016/j.matt.2022.07.028.
(13) FitzGerald, L. I.; Olorunyomi, J. F.; Singh, R.; Doherty, C. M. Towards Solving the PFAS Problem: The Potential Role of Metal-Organic Frameworks. *ChemSusChem* **2022**, *15* (19). DOI: 10.1002/cssc.202201136.
(14) Liu, K.; Zhang, S.; Hu, X.; Zhang, K.; Roy, A.; et al. Understanding the Adsorption of PFOA on MIL-101(Cr)-Based Anionic-Exchange Metal–Organic Frameworks: Comparing

DFT Calculations with Aqueous Sorption Experiments. *Environ. Sci. Technol.* **2015**, *49* (14), 8657-8665. DOI: 10.1021/acs.est.5b00802.
(15) Yang, Y.; Zheng, Z.; Ji, W.; Xu, J.; Zhang, X. Insights to perfluorooctanoic acid adsorption micro-mechanism over Fe-based metal organic frameworks: Combining computational calculation with response surface methodology. *J. Hazard. Mater.* **2020**, *395* (122686). DOI: 10.1016/j.jhazmat.2020.122686.
(16) Boontongto, T.; Burakham, R. Evaluation of metal-organic framework NH2-MIL-101(Fe) as an efficient sorbent for dispersive micro-solid phase extraction of phenolic pollutants in environmental water samples. *Heliyon* **2019**, *5* (11). DOI: 10.1016/j.heliyon.2019.e02848.
(17) Chen, M. J.; Yang, A. C.; Wang, N. H.; Chiu, H. C.; Li, Y. L.; et al. Influence of crystal topology and interior surface functionality of metal-organic frameworks on PFOA sorption performance. *Micropor. Mesopor. Mat.* **2016**, *236*, 202-210. DOI: 10.1016/j.micromeso.2016.08.046.
(18) Li, Y.; Yang, Z.; Wang, Y.; Bai, Z.; Zheng, T.; et al. A mesoporous cationic thorium-organic framework that rapidly traps anionic persistent organic pollutants. *Nat. Commun.* **2017**, *8* (1). DOI: 10.1038/s41467-017-01208-w.
(19) Clark, C. A.; Heck, K. N.; Powell, C. D.; Wong, M. S. Highly Defective UiO-66 Materials for the Adsorptive Removal of Perfluorooctanesulfonate. *ACS Sustain. Chem. Eng.* **2019**, *7* (7), 6619-6628. DOI: 10.1021/acssuschemeng.8b05572.
(20) Sini, K.; Bourgeois, D.; Idouhar, M.; Carboni, M.; Meyer, D. Metal–organic framework sorbents for the removal of perfluorinated compounds in an aqueous environment. *New J. Chem.* **2018**, *42* (22). DOI: 10.1039/C8NJ03312A.
(21) Li, R.; Alomari, S.; Stanton, R.; Wasson, M. C.; Islamoglu, T.; et al. Efficient Removal of Per- and Polyfluoroalkyl Substances from Water with Zirconium-Based Metal–Organic Frameworks. *Chem. Mater.* **2021**, *33* (9). DOI: 10.1021/acs.chemmater.1c00324.
(22) Suwannakot, P.; Lisi, F.; Ahmed, E.; Liang, K.; Babarao, R.; et al. Metal–Organic Framework-Enhanced Solid-Phase Microextraction Mass Spectrometry for the Direct and Rapid Detection of Perfluorooctanoic Acid in Environmental Water Samples. *Anal. Chem.* **2020**, *92* (10), 6900-6908. DOI: 10.1021/acs.analchem.9b05524.
(23) Jia, Y.; Qian, J.; Pan, B. Dual-Functionalized MIL-101(Cr) for the Selective Enrichment and Ultrasensitive Analysis of Trace Per- and Poly-fluoroalkyl Substances. *Anal. Chem.* **2021**, *93* (32), 11116-11122. DOI: 10.1021/acs.analchem.1c01489.
(24) Yang, X.; Lin, Z.; Yan, X.; Cai, Z. Zeolitic imidazolate framework nanocrystals for enrichment and direct detection of environmental pollutants by negative ion surface-assisted laser desorption/ionization time-of-flight mass spectrometry. *RSC Adv.* **2016**, *6* (28), 23790-23793. DOI: 10.1039/C6RA00877A.
(25) Ma, S. Y.; Wang, J.; Fan, L.; Duan, H. L.; Zhang, Z. Q. Preparation of a fluorinated metal-organic framework and its application for the dispersive solid-phase extraction of perfluorooctanoic acid. *J. Chromatogr. A* **2020**, *1611* (460616). DOI: 10.1016/j.chroma.2019.460616.
(26) Wang, S.; Niu, H.; Zeng, T.; Zhang, X.; Cao, D.; et al. Rapid determination of small molecule pollutants using metal-organic frameworks as adsorbent and matrix of MALDI-TOF-MS. *Micropor. Mesopor. Mater.* **2017**, *239*, 390-395. DOI: 10.1016/j.micromeso.2016.10.032.
(27) Deacon, A.; Briquet, L.; Malankowska, M.; Massingberd-Mundy, F.; Rudić, S.; et al. Understanding the ZIF-L to ZIF-8 transformation from fundamentals to fully costed kilogram-scale production. *Comm. Chem.* **2022**, *5* (1). DOI: 10.1038/s42004-021-00613-z.
(28) Gu, Y.; Li, X.; Ye, G.; Gao, Z.; Xu, W.; et al. Accelerated and scalable synthesis of UiO-66(Zr) with the assistance of inorganic salts under solvent-free conditions. *New J. Chem.* **2021**, *45* (21). DOI: 10.1039/D1NJ01059J.

(29) Zhang, H.; Zhao, M.; Lin, Y. S. Stability of ZIF-8 in water under ambient conditions. *Micropor. Mesopor. Mat.* **2019**, *279*. DOI: 10.1016/j.micromeso.2018.12.035.
(30) Bůžek, D.; Demel, J.; Lang, K. Zirconium Metal–Organic Framework UiO-66: Stability in an Aqueous Environment and Its Relevance for Organophosphate Degradation. *Inorg. Chem.* **2018**, *57* (22). DOI: 10.1021/acs.inorgchem.8b02360.
(31) Lee, Y.-R.; Do, X. H.; Hwang, S. S.; Baek, J.-Y. Dual-functionalized ZIF-8 as an efficient acid-base bifunctional catalyst for the one-pot tandem reaction. *Catal. Today* **2021**, *359*, 124-132. DOI: 10.1016/j.cattod.2019.06.076.
(32) Lee, Y. R.; Do, X. H.; Cho, K. Y.; Jeong, K.; Baek, K.-Y. Amine-Functionalized Zeolitic Imidazolate Framework-8 (ZIF-8) Nanocrystals for Adsorption of Radioactive Iodine. *ACS Appl. Nano Mater.* **2020**, *3* (10). DOI: 10.1021/acsanm.0c01914.
(33) Cho, K. Y.; An, H.; Do, X. H.; Choi, K.; Yoon, H. G.; et al. Synthesis of amine-functionalized ZIF-8 with 3-amino-1,2,4-triazole by postsynthetic modification for efficient CO2-selective adsorbents and beyond. *J. Mater. Chem. A* **2018**, *6* (39). DOI: 10.1039/C8TA02797H.
(34) DeCoste, J. B.; Peterson, G. W.; Jasuja, H.; Glover, T. G.; Huang, Y.-g.; et al. Stability and degradation mechanisms of metal–organic frameworks containing the Zr6O4(OH)4 secondary building unit. *J. Mater. Chem. A* **2013**, *1* (18). DOI: 10.1039/C3TA10662D.
(35) Cavka, J. H.; Jakobsen, S.; Olsbye, U.; Guillou, N.; Lamberti, C.; et al. A New Zirconium Inorganic Building Brick Forming Metal Organic Frameworks with Exceptional Stability. *J. Am. Chem. Soc.* **2008**, *130* (42). DOI: 10.1021/ja8057953.
(36) Zhao, W.; Zhang, C.; Yan, Z.; Zhou, Y.; Li, J.; et al. Preparation, characterization, and performance evaluation of UiO-66 analogues as stationary phase in HPLC for the separation of substituted benzenes and polycyclic aromatic hydrocarbons. *PLoS One* **2017**, *12* (6). DOI: 10.1371/journal.pone.0178513.
(37) Ethiraj, J.; Albanese, E.; Civalleri, B.; Vitillo, J. G.; Bonino, F.; et al. Carbon Dioxide Adsorption in Amine-Functionalized Mixed-Ligand Metal–Organic Frameworks of UiO-66 Topology. *ChemSusChem* **2014**, *7* (12). DOI: 10.1002/cssc.201402694.
(38) Park, K. S.; Ni, Z.; Côté, A. P.; Choi, J. Y.; Huang, R.; et al. Exceptional chemical and thermal stability of zeolitic imidazolate frameworks. *Proc. Natl. Acad. Sci.* **2006**, *103* (27). DOI: 10.1073/pnas.0602439103.
(39) Shearer, G. C.; Chavan, S.; Ethiraj, J.; Vitillo, J. G.; Svelle, S.; et al. Tuned to Perfection: Ironing Out the Defects in Metal–Organic Framework UiO-66. *Chem. Mater.* **2014**, *26* (14), 4068-4071. DOI: 10.1021/cm501859.
(40) Shi, G.; Xie, Y.; Guo, Y.; Dai, J. 6:2 fluorotelomer sulfonamide alkylbetaine (6:2 FTAB), a novel perfluorooctane sulfonate alternative, induced developmental toxicity in zebrafish embryos. *Aquat. Toxicol.* **2018**, *195*, 24-32. DOI: 10.1016/j.aquatox.2017.12.002.
(41) Bianca Ferreira da Silva; Juan J Aristizabal-Henao; Joe Aufmuth; Jill Awkerman; Bowden, J. A. Survey of per- and polyfluoroalkyl substances (PFAS) in surface water collected in Pensacola, FL. *Heliyon* **2022**, *8* (8). DOI: 10.1016/j.heliyon.2022.e10239.
(42) Brunauer, S.; Emmett, P. H.; Teller, E. Adsorption of Gases in Multimolecular Layers. *J. Am. Chem. Soc.* **1938**, *60* (2). DOI: 10.1021/ja01269a023.